Int J Clin Exp Med 2016;9(12):23039-23047
www.ijcem.com /ISSN:1940-5901/IJCEM0030184

Original Article

MicroRNA-130a promotes apoptosis of alveolar epithelia in COPD patients by inhibiting autophagy via the down-regulation of ATG16L expression

Zhanying Li, Na Han, Yanqing Tian

Department of Tuberculosis, Affiliated Hospital of Hebei University, Baoding 071000, P. R. China

Received April 9, 2016; Accepted October 26, 2016; Epub December 15, 2016; Published December 30, 2016

Abstract: Aims: The present study is to investigate the expression of microRNA (miR)-130a in chronic obstructive pulmonary disease (COPD) tissues, as well as its function and potential mechanism. Methods: A total of 43 patients with COPD who received lobectomy due to pulmonary bulla at our hospital between August 2012 and January 2015 were included in the present study. Tissues at the foci and those more than 5 cm away from the foci were included into COPD and normal control groups, respectively. Quantitative real-time polymerase chain reaction was used to measure the expression of miR-130a. After transfection with miR-130a mimics, Cell-Counting Kit 8 assay and flow cytometry, were used to study the proliferation, cell cycle and apoptosis of primary human pulmonary alveolar epithelial cells (HPAEpiCs). Western blotting was used to measure the expression of ATG16L and electron microscopy was used to study the autophagy of HPAEpiCs. Dual luciferase reporter assay was carried out to identify the direct binding between ATG16L and miR-130a. Results: Expression of miR-130a was elevated in COPD tissues. Overexpression of miR-130a inhibited the proliferation of HPAEpiCs possibly by controlling the transition between G1 and S phases. Overexpression of miR-130a facilitated the apoptosis of HPAEpiCs and aggravated damages in the lungs. miR-130a regulated the expression of ATG16L that exerted its biological effect by facilitating the apoptosis of HPAEpiCs. miR-130a reduced autophagy activity of HPAEpiCs by targeting ATG16L. Conclusions: The present study demonstrates that the expression of miR-130a in COPD tissues is elevated, and miR-130a facilitates the occurrence and development of COPD by inhibiting autophagy and promoting apoptosis of HPAEpiCs.

Keywords: MicroRNA-130a, chronic obstructive pulmonary disease, autophagy, apoptosis, human pulmonary alveolar epithelial cells

Introduction

Chronic obstructive pulmonary disease (COPD) is a common disease in respiratory system that is characterized by incompletely reversible airflow limitation and progressive development [1]. According to World Health Organization, the mortality rate of COPD is the fourth highest cause of death among all diseases, greatly threatening human health [2]. The pathogenesis of COPD is very complicated. At present, it is widely accepted that sustained inflammatory response, oxidative stress, repair of damaged cells, cell death, the destruction of extracellular matrix, and cell apoptosis in airway structure are closely related to the occurrence and development of COPD [3, 4]. The main pathological manifestation of COPD is obstructive emphysema, which is characterized by expansion of air cavity in the distal end of terminal bronchioles, alveolar wall defect, reduction of alveolar units, and decrease of alveolar septal cells. The structural cells of alveolar septum are attracting more and more attention from researchers, including alveolar epithelial cells and pulmonary vascular endothelial cells. Especially, the effect of alveolar epithelial cells in the formation of emphysema has attracted most of the concerns [5, 6].

MicroRNA (miRNA or miR) is a kind of non-encoding small RNA molecules with lengths of 18-23 nucleotides. miRNA can bind the 3'-untranslated region (UTR) of the mRNA of target genes, form silenced protein complex, and regulate the expression of target genes post-transcriptionally. miRNA participates in nearly all physiological and pathological processes of

eukaryotic cells [7]. It is discovered that disordered miRNA expression exists in lung tissue or peripheral blood of COPD patients, and a variety of miRNA molecules play important roles in the occurrence and development of COPD [8]. For example, miR-203 promotes the progression of COPD by regulating PI3K signaling pathway [9]. In addition, miR-1343 affects pulmonary remodeling in patients with COPD by regulating the expression of TGF-β receptors [10]. miR-130 is a newly discovered miRNA molecule that is closely related with tumors, cardiovascular diseases and pulmonary arterial hypertension [11, 12]. Specific overexpression of miR-130a in cardiomyocytes causes ventricular hypertrophy and ventricular septal defect in mice [13]. miR-130a promotes the proliferation, invasion and metastasis of bladder cancer cells by regulating PTEN signaling pathway [14]. By now, studies on the expression and mechanism of action of miR-130a are never reported. In the present study, we investigate the effect of miR-130a on human pulmonary alveolar epithelial cells (HPAEpiCs) at tissue and cellular levels, as well as its molecular mechanism.

Materials and methods

Patients

A total of 43 patients with COPD who received lobectomy due to pulmonary bulla at our hospital between August 2012 and January 2015 were included in the present study. The 43 patients included 31 males and 12 females with an average age of 64.3 ± 4.2 years. None of the patients had other acute and chronic diseases such as acute respiratory distress syndrome, bronchial asthma, idiopathic pulmonary fibrosis and connective tissue disease-associated pulmonary fibrosis. The course of disease of COPD was divided into acute exacerbation period and stable period according to clinical symptoms. In acute exacerbation period, patients had aggravated cough, expectoration, shortness of breath and wheezing, increased sputum, purulent or mucopurulent symptoms, or fever. In stable period, the patients had stable or mild symptoms of cough, expectoration, or shortness of breath. Among the patients in the present study, 11 patients were in acute exacerbation period and 32 were in stable period. Of note, the expression of miR-130a was not significantly different between the two groups of patients. Gender, age, and pulmonary function status of the patients were recorded. Resected tissues that are more than 5 cm away from the foci were used as normal control. Percentage of forced expiratory volume in the first second over predicted value (FEV1% pre) was 64.70 ± 4.80%. Forced expiratory volume in the first second/forced vital capacity (FEV1/FVC) was 65.40 ± 3.74%. Residual volume/total lung capacity (RV/TLC) was 43.97 ± 6.21%. Under the microscope, the alveolar septum became thinner and broken, and the alveolar cavity was enlarged. All procedures were approved by the Ethics Committee of Hebei University. Written informed consents were obtained from all patients or their families.

Cells

Primary HPAEpiCs were purchased from Scien Cell Research Laboratories (Carlsbad, CA, USA) and cultured in Dulbecco's modified Eagle medium supplemented with 10% fetal bovine serum at 37°C and 5% CO_2. The medium was refreshed every two days. When reaching a confluency of 90%, the cells were passaged. Cells with passage numbers of 3, 4, and 5 were used for experiments.

After seeding the cells into 24-well plates, the cells were divided into control group, negative control group (miR-NC) and miR-130a mimics group. Before transfection, 1.25 μl miR-130a mimics (20 μM) and 1 μl Lipofectamine 2000 (Thermo Fisher Scientific, Waltham, MA, USA) were added into two individual vials containing 50 μl OptiMemi medium, respectively. Five minutes later, the liquids in the two vials were mixed before standing still for another 15 min. Then, the mixture was added onto cells with a confluency of 70-90% in miR-130a mimics group before incubation for 6 h. After changing fresh medium, the cells were cultured under normal condition for 24 h. To silence the expression of ATG16L, siRNA was co-transfected with ATG16L using the same method.

Quantitative real-time polymerase chain reaction (qRT-PCR)

Before total RNA extraction, tissues (100 mg) were ground into powder using liquid nitrogen before addition of 1 ml Trizol (Thermo Fisher Scientific, Waltham, MA, USA) for lysis. Afterwards, total RNA was extracted using phenol

chloroform method. Then, cDNA was obtained by reverse transcription by the addition of polyA tail and stored at -20°C. U6 was used as internal reference. PCR reaction system (30 μl) included 10 μl PCR mix, 0.5 μl upstream primer, 0.5 μl downstream primer, 5 μl cDNA and 14 μl H_2O. The upstream primer was 5'-CAGTGCAATGTTAAAAGGGCA-3', and downstream primer was a universal primer. PCR conditions were: initial denaturation at 95°C for 10 min, and 40 cycles of denaturation at 95°C for 30 s and annealing at 60°C for 30 s. Quantitative measurements were performed using the $2^{-\Delta\Delta Ct}$ method. All samples were measured in triplicate.

Cell-Counting Kit 8 (CCK-8) assay

For growth curve assay, cells were seeded into 96-well plates at a density of 3,000 cells per well in triplicate. Every 24 hours, the cells were incubated with CCK-8 reagent for 30 min. Absorbance at 490 nm was read on a microplate reader (168-1000; Model 680, Bio-Rad, Hercules, CA, USA) at 24 h, 48 h, and 72 h, and proliferation curves were plotted using absorbance values at each time point.

Flow cytometry

At 24 h after transfection with miR-130a mimics, 1×10^6 cells were washed with pre-cooled phosphate-buffered saline twice before being subjected to the detection of cell cycle using Cell Cycle Assay Kit (BD Biosciences, Franklin Lakes, NJ, USA) following the manufacturer's manual. The cells were incubated with 200 μl fluid A at room temperature for 10 min, and then 150 μl fluid B at room temperature for 10 min. At last, 120 μl fluid C was added, followed by incubation in dark for 10 min. Then, flow cytometry was performed and ModFit software was used for analysis.

At 48 h after transfection with miR-130a mimics, 1×10^6 cells were washed with pre-cooled phosphate-buffered saline for three times before being subjected to the detection of apoptosis using ANXN V FITC APOPTOSIS DTEC KIT I (BD Biosciences, Franklin Lakes, NJ, USA) following the manufacturer's manual. Cells with positive Annexin-V staining only were early apoptotic cells, those only positively stained with propidium iodide were necrotic cells, while those with double staining by Annexin-V and propidium iodide were late apoptotic cells. Apoptotic index was obtained from the percentage of cells double-stained by Annexin-V/propidium iodide. Each test was performed in triplicate.

Western blotting

ATG16L and LC3B expression was determined using Western blotting. At 48 h after transfection, total protein was extracted from the cells using radioimmunoprecipitation assay lysis buffer containing 1% phenylmethylsulfonyl fluoride. The resulted protein (20 μg) was loaded onto sodium dodecyl sulfate polyacrylamide gel (100 g/L) for electrophoresis and then transferred onto polyvinylidene fluoride membrane. After blocking with skimmed milk (50 g/L) for 2 h, rabbit anti-human polyclonal ATG16L primary antibody (1:1,000; Abcam, Cambridge, UK) and rabbit anti-human polyclonal LC3B primary antibody (1:1,000; Abcam, Cambridge, UK) were added for incubation at 4°C overnight. On the next day, goat anti-rabbit horseradish peroxidase-labelled secondary antibody (1:1,000; Abcam, Cambridge, UK) was added for incubation at room temperature for 1.5 h. The membrane was washed with Tris-buffered saline with Tween 20. Immunoreactive bands were detected using electrochemiluminescence reagent kit (Thermo Fisher Scientific, Waltham, MA, USA). The relative band densities were analyzed using Image-Pro Plus v7.0 (Media Cybernetics, Bethesda, MD, USA).

Electron microscopy

Samples were fixed in 2.5% glutaraldehyde in 0.1 M phosphate-buffered saline (PBS), washed three times for 10 minutes in PBS, post-fixed for 30 min in 1% osmium tetroxide at 4°C, and washed three more times in PBS. After dehydration through a graded ethanol series (50%, 70%, 90% and 100%; 10 min each), samples were soaked in 2 ml pure acetone-EPON812 embedding agent (v/v, 1:1) for 30 min. After discarding embedding agent, the samples were soaked with 1 ml pure embedding agent for 2 min at room temperature. After baking the samples at 60°C for 2 h, the samples were mounted on microtome to obtain slices with thicknesses of 50-70 nm. The slices were stained with sodium acetate for 5-30 min and washed with water for 3 times. After staining with lead citrate, the slices were examined under a scan-

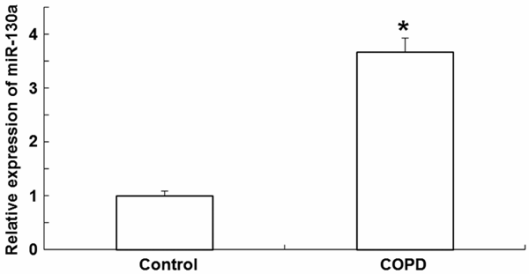

Figure 1. Expression of miR-130a in COPD tissues. qRT-PCR was used to measure the level of miR-130a. *P < 0.05 compared with control.

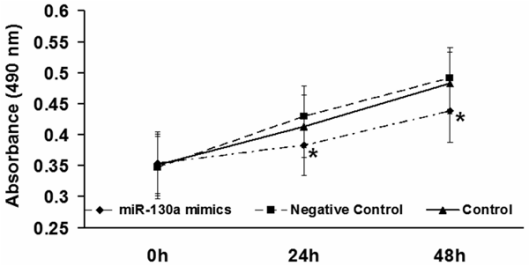

Figure 2. Effect of miR-130a overexpression on the proliferation of HPAEpiCs. CCK-8 assay was used to detect cell proliferation. *P < 0.05 compared with control and negative control.

ning electron microscope (Verios XHR Scanning Electron Microscope, FEI, Hillsboro, OR, USA).

Dual luciferase reporter assay

The potential target genes of miR-130a were predicted using bioinformatics. miR-130a was identified to be capable of binding with 3'-UTR of ATG16L mRNA. ATG16L gene expression was interfered by small interfering RNA. According to bioinformatics results, wild-type (WT) and mutant seed regions of miR-130a in the 3'-UTR of ATG16L gene were chemically synthesized in vitro, added with Spe-1 and HindIII restriction sites, and then cloned into pMIR-REPORT luciferase reporter plasmids. Plasmids (0.5 μg) with WT or mutant 3'-UTR DNA sequences were co-transfected with miR-130a mimics into HEK-293T cells. After cultivation for 24 h, the cells were lysed using dual luciferase reporter assay kit (Promega, Fitchburg, WI, USA) according to the manufacturer's manual, and fluorescence intensity was measured using GloMax 20/20 luminometer (Promega, Fitchburg, WI, USA). Using renilla fluorescence activity as internal reference, the fluorescence values of each group of cells were measured.

Statistical analysis

The results were analyzed using SPSS 16.0 statistical software (IBM, Armonk, NY, USA). All measurement data were expressed as means ± standard deviation. Intergroup comparison was performed using group t-test. Differences with $P < 0.05$ were considered statistically significant.

Results

Expression of miR-130a is elevated in COPD tissues

To measure the level of miR-130a in COPD tissues, qRT-PCR was carried out. The data showed that miR-130a expression in COPD tissues was significantly higher than in control ($P < 0.05$) (**Figure 1**). The result suggests that expression of miR-130a is elevated in COPD tissues.

Overexpression of miR-130a inhibits the proliferation of HPAEpiCs

To study the proliferation of HPAEpiCs, CCK-8 assay was performed. The data showed that the proliferation of HPAEpiCs in miR-130a mimics group was significantly decreased compared with those in control and miR-NC groups at 24 h or 48 h ($P < 0.05$) (**Figure 2**). The result indicates that overexpression of miR-130a inhibits the proliferation of HPAEpiCs.

Increased miR-130a expression inhibits the proliferation of HPAEpiCs possibly by controlling the transition between G1 and S phases

To detect the cell cycle of HPAEpiCs, flow cytometry was employed. The data showed that HPAEpiCs in miR-130a mimics group had G1/S phase arrestment (**Figure 3**). The result suggests that increased miR-130a expression inhibits the proliferation of HPAEpiCs possibly by controlling the transition between G1 and S phases.

Overexpression of miR-130a facilitates the apoptosis of HPAEpiCs and aggravates damages in the lungs

To detect HPAEpiCs apoptosis, flow cytometry was carried out. The data showed that the apoptotic rate of HPAEpiCs in miR-130a mimics group was significantly higher than that in miR-

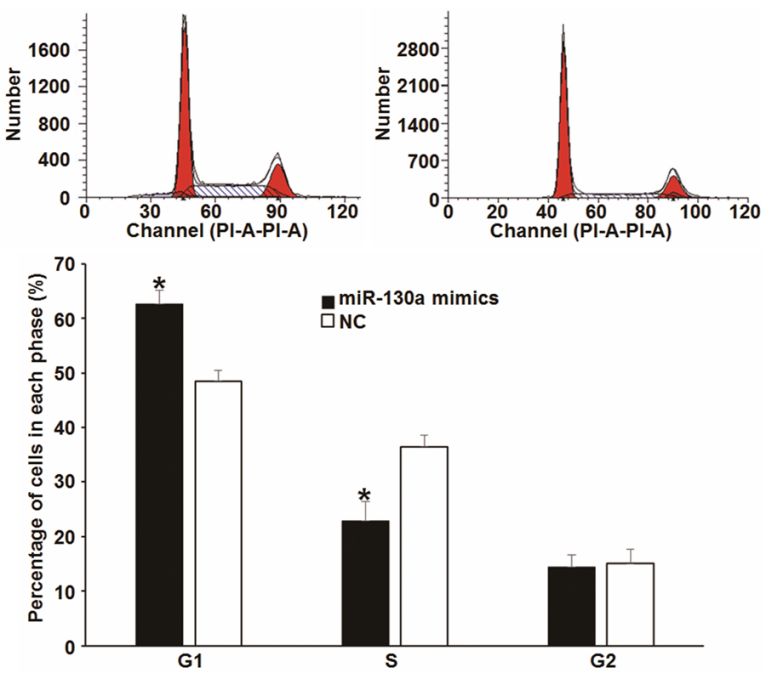

Figure 3. Effect of miR-130a overexpression on cell cycle of HPAEpiCs. Cell cycle was detected using flow cytometry. The percentages of cells in G1, S, and G2 phases were determined. *P < 0.05 compared with NC group.

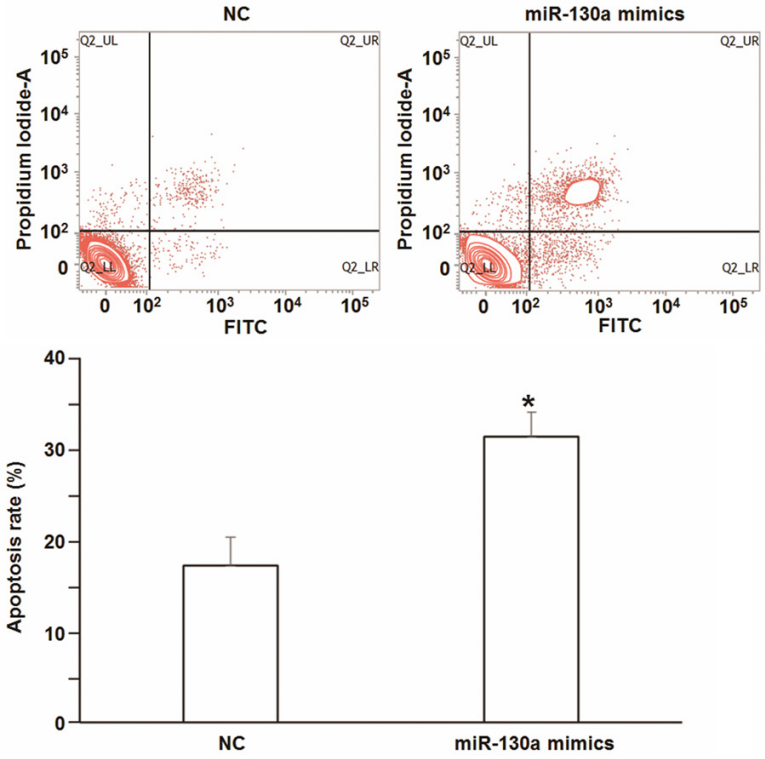

Figure 4. Effect of miR-130a overexpression on apoptosis of HPAEpiCs. Apoptosis was detected using flow cytometry. *P < 0.05 compared with NC.

NC group (P < 0.05) (**Figure 4**). The result indicates that overexpression of miR-130a facilitates the apoptosis of HPAEpiCs and aggravates damages in the lungs.

miR-130a regulates the expression of ATG16L that exerts its biological effect by facilitating the apoptosis of HPAEpiCs

To test whether miR-130a regulates the expression of antophagy-related gene ATG16L, Western blotting was used. The data showed that overexpression of miR-130a decreased the expression of ATG16L protein in HPAEpiCs (P < 0.05) (**Figure 5A**). In addition, silencing of ATG16L by co-transfection with siRNA decreased the expression of ATG16L (**Figure 5B**), failed to alter the proliferation of HPAEpiCs (P > 0.05) (data not shown), and significantly enhanced the apoptosis of the cells (P < 0.05) (**Figure 5C**). The results suggest that miR-130a regulates the expression of ATG16L that exerts its biological effect by facilitating the apoptosis of HPAEpiCs.

miR-130a reduces autophagy activity of HPAEpiCs by targeting ATG16L

To observe autophagy of HPAEpiCs, electron microscopy and Western blotting were adopted. Western blotting analysis showed that the ratio of type I LC3B protein to type II LC3B protein in miR-130a mimics group was significantly greater than that in miR-NC group (P < 0.05) (**Figure 6A**). Similarly, silencing of ATG16L by co-transfection with siRNA significantly increased the ratio of type I LC3B protein to type II LC3B protein (**Figure 6B**). Electron microscopy showed that the number of autophagosomes in miR-130a mimics group was lower than that in miR-NC group (P < 0.05)

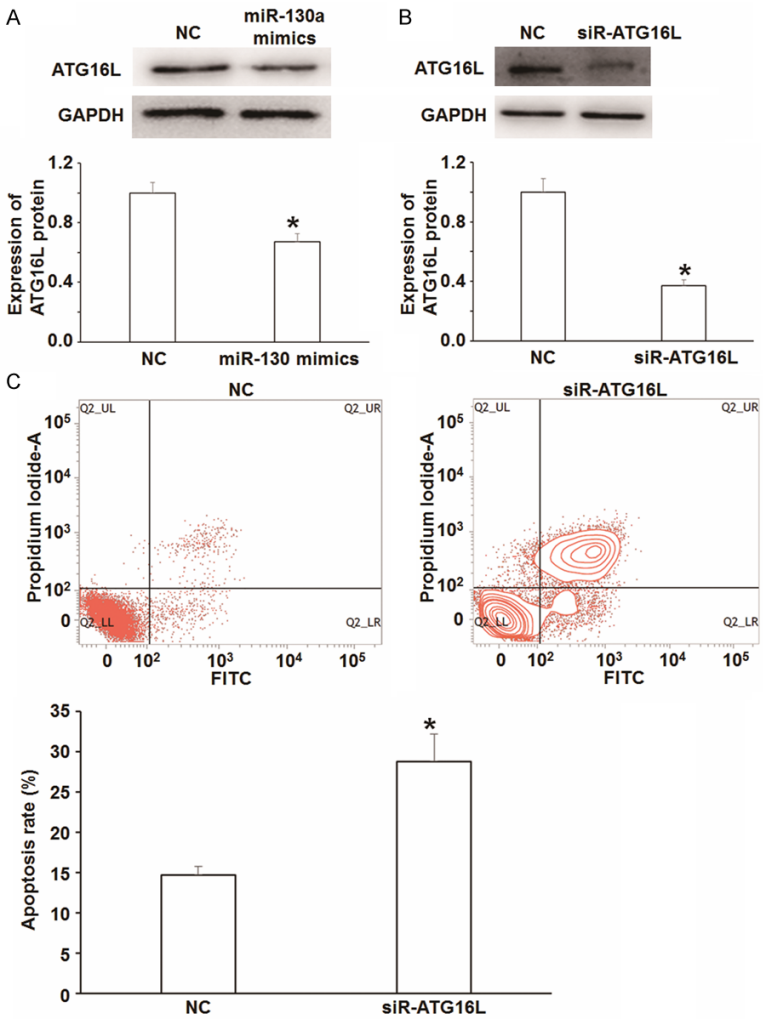

Figure 5. The relationship among miR-130a overexpression, ATG16L expression and the apoptosis of HPAEpiCs. A. Effect of miR-130a overexpression on the expression of ATG16L. B. Effect of co-transfection with siRNA of ATG16L on the expression of ATG16L. C. Effect of silencing of ATG16L on the apoptosis of HPAEpiCs. *P < 0.05 compared with NC.

(**Figure 6C**). Consistently, the number of autophagosomes in siR-ATG16L group was reduced compared with that in miR-NC group (P < 0.05) (**Figure 6D**). These results indicate that miR-130a reduces autophagy activity of HPAEpiCs by targeting ATG16L.

miR-130a is able to bind with 3'-UTR of the mRNA of its target gene ATG16L1

To confirm interactions between miR-130a and 3'-UTR of ATG16L1 gene, dual luciferase reporter assay was carried out. The data showed that fluorescence values of cells co-transfected with miR-130a mimics and pMIR-REPORT-WT plasmids were significantly lower than control (P < 0.05), while those of cells co-transfected with miR-130a mimics and pMIR-REPORT-mutant plasmids were not different from control (P > 0.05) (**Figure 7**). The result indicates that miR-130a is able to bind with 3'-UTR of the mRNA of its target gene ATG16L1.

Discussion

Our results show that expression of miR-130a is significantly elevated in COPD tissues, suggesting that it may have important biological functions in the occurrence and development of COPD. In addition, miR-130a down-regulates the expression of ATG16L gene, inhibits the proliferation and autophagy ability of HPAEpiCs, promotes the apoptosis of HPAEpiCs, and aggravates injuries in lung tissues of COPD patients. These results demonstrate that miR-130a facilitates the occurrence and development of COPD, aggravates injuries in the lungs, and may be a potential clinical diagnosis and therapeutic target.

It is reported that the proliferation, apoptosis and necrosis of alveolar epithelial cells have a dynamic balance that maintains the integrity of alveolar septal structure and function [15]. In COPD, this balance in alveolar epithelial cells is broken, the proliferation of these cells is abnormal, and apoptosis and necrosis are increased, leading to disrupted alveolar septal structure and function, as well as aggravated COPD [16]. In this process, miRNA plays important regulatory roles. For example, miR-203 promotes the apoptosis of alveolar epithelial cells by regulating PI3K signaling pathway [17], and miR-124 participates in the regulation of local immune response that leads to alveolar epithelial cell injury [18]. In the present study, we have detected elevated expression of miR-130a in COPD tissues, suggesting that miR-

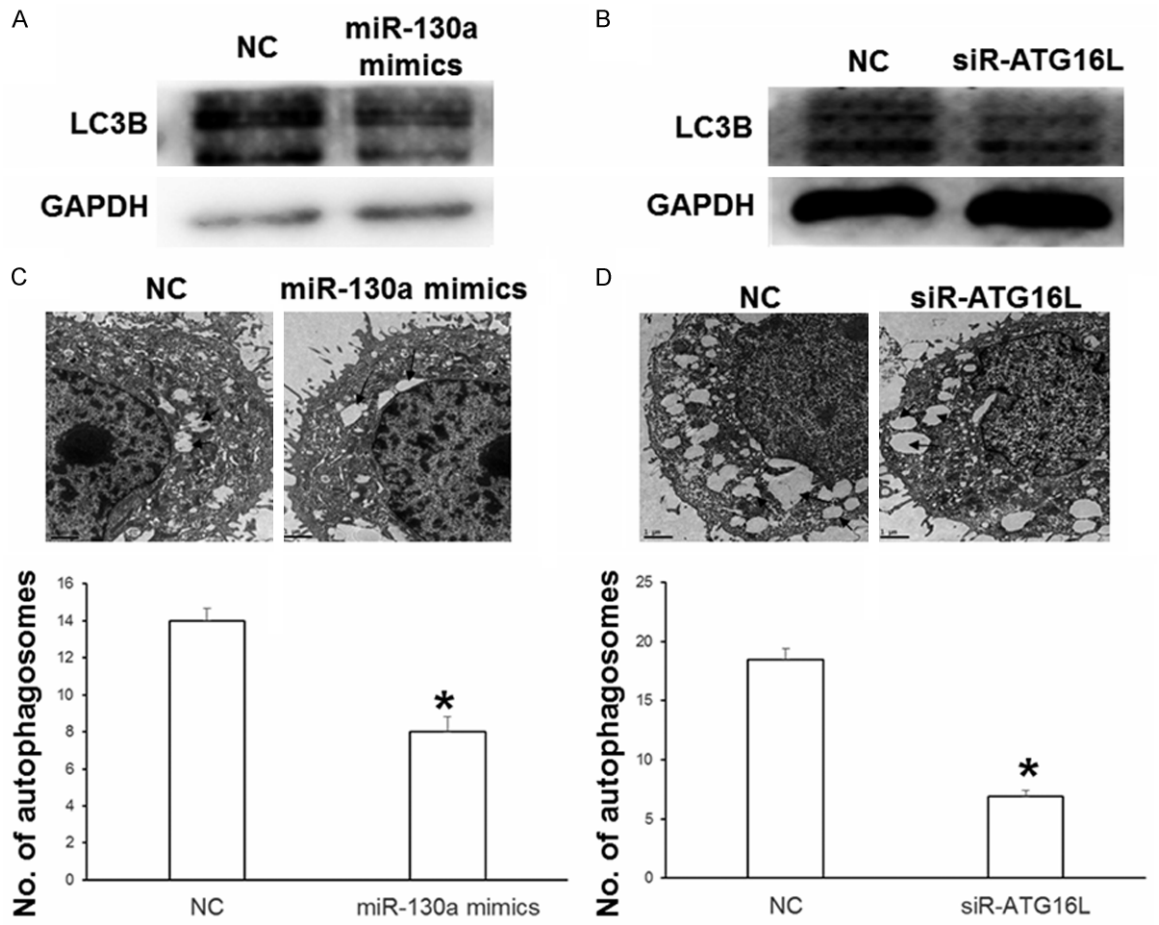

Figure 6. Effect of miR-130a on autophagy of HPAEpiCs. A. Effect of miR-130a overexpression on the expression of LC3B. B. Effect of co-transfection with siRNA of ATG16L on the expression of LC3B. C. Effect of miR-130a overexpression on the number of autophagosomes in HPAEpiCs. D. Effect of silencing of ATG16L on the number of autophagosomes in HPAEpiCs. *P < 0.05 compared with NC.

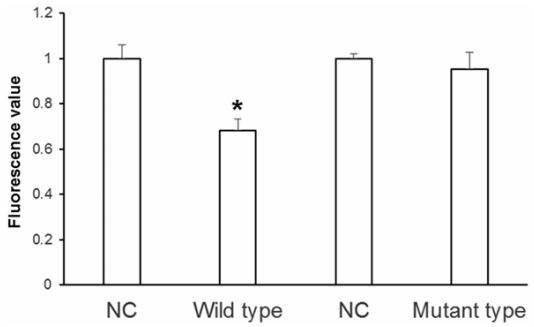

Figure 7. Interactions between miR-130a and 3'-UTR of ATG16L1 gene. Dual luciferase reporter assay was used to measure fluorescence value that identifies the direct binding of miR-130a with 3'-UTR of ATG16L1. *P < 0.05 compared with NC.

130a may participates in the development of COPD. In vitro experiments show that miR-130a inhibits the proliferation of HPAEpiCs, and promotes the apoptosis of HPAEpiCs. Bioinformatics prediction finds that miR-130a may regulate autophagy-related ATG16L gene, which can activate the autophagy of cells. Studies show that autophagy is closely related with cell apoptosis, proliferation, and epithelial-mesenchymal transition, and has complex crosstalk with apoptosis signaling pathway [19-21]. Our Western blotting and electron microscopy data show that transfection with miR-130a inhibits autophagy activity of cells, increases the ratio of type I LC3B protein to type II LC3B protein, and reduces the number of intracellular antophagosomes. Moreover, interference of ATG16L expression using siRNA elevates apoptotic rate of HPAEpiCs and the ratio of type I LC3B protein to type II LC3B protein, and decreases the number of autophago-

somes in the cells. Of note, dual luciferase reporter assay has identified direct binding of miR-130a with the 3'-UTR of ATG16L. In conclusion, high expression of miR-130a is closely related with the occurrence and development of COPD. On one hand, miR-130a directly inhibits the proliferation of alveolar epithelial cells, and reduces their self-repair ability. On the other hand, miR-130a regulates the expression of ATG16L, inhibits autophagy activity of cells, promotes the apoptosis of alveolar epithelial cells, aggravates alveolar septal injuries, and promotes the development of COPD. Inhibition of miR-130a expression may alleviate or delay the progression of COPD, and miR-130a can be a potential drug therapeutic target.

Acknowledgements

We would like to thank Professor Haisong Zhang, the President of the Hospital, and Professor Shujie Cheng, the Director of the Department, for their valuable help and support.

Disclosure of conflict of interest

None.

Address correspondence to: Na Han, Department of Tuberculosis, Affiliated Hospital of Hebei University, No. 648 East Dongfeng Road, Baoding 071000, Hebei, P. R. China. Tel: 86-18903363913; E-mail: hn0008@126.com

References

[1] Yawn BP. Microbiome in asthma and COPD. J Fam Pract 2016; 65.

[2] Su VY, Chang YS, Hu YW, Hung MH, Ou SM, Lee FY, Chou KT, Yang KY, Perng DW, Chen TJ and Liu CJ. Carvedilol, bisoprolol, and metoprolol use in patients with coexistent heart failure and chronic obstructive pulmonary disease. Medicine (Baltimore) 2016; 95: e2427.

[3] Labonte LE, Tan WC, Li PZ, Mancino P, Aaron SD, Benedetti A, Chapman KR, Cowie R, FitzGerald JM, Hernandez P, Maltais F, Marciniuk DD, O'Donnell D, Sin D, Bourbeau J; Canadian Respiratory Research N and the Can CCRg. Undiagnosed COPD contributes to the burden of health care utilization: data from the can COLD study. Am J Respir Crit Care Med 2016; [Epub ahead of print].

[4] Uyanaeva AI, Airapetova NS, Badalov NG, Tupitsina YY, L'Vova NV, Nitchenko OV, Uyanaeva MA and Ksenofontova IV. The role of physiobalneotherapy in the prevention of weather-dependent exacerbations in the patients presenting with chronic obstructive pulmonary disease. Vopr Kurortol Fizioter Lech Fiz Kult 2015; 92: 17-22.

[5] Mandal S, Suh E, Thompson A, Connolly B, Ramsay M, Harding R, Puthucheary Z, Moxham J and Hart N. Comparative study of linear and curvilinear ultrasound probes to assess quadriceps rectus femoris muscle mass in healthy subjects and in patients with chronic respiratory disease. BMJ Open Respir Res 2016; 3: e000103.

[6] Faisy C, Meziani F, Planquette B, Clavel M, Gacouin A, Bornstain C, Schneider F, Duguet A, Gibot S, Lerolle N, Ricard JD, Sanchez O, Djibre M, Ricome JL, Rabbat A, Heming N, Urien S, Esvan M and Katsahian S. Effect of acetazolamide vs placebo on duration of invasive mechanical ventilation among patients with chronic obstructive pulmonary disease: a randomized clinical trial. JAMA 2016; 315: 480-488.

[7] Leidinger P, Brefort T, Backes C, Krapp M, Galata V, Beier M, Kohlhaas J, Huwer H, Meese E and Keller A. High-throughput qRT-PCR validation of blood microRNAs in non-small cell lung cancer. Oncotarget 2016; 7: 4611-4623.

[8] Hubenthal M, Hemmrich-Stanisak G, Degenhardt F, Szymczak S, Du Z, Elsharawy A, Keller A, Schreiber S and Franke A. Sparse modeling reveals miRNA signatures for diagnostics of inflammatory bowel disease. PLoS One 2015; 10: e0140155.

[9] Shi L, Xin Q, Chai R, Liu L and Ma Z. Ectopic expressed miR-203 contributes to chronic obstructive pulmonary disease via targeting TAK1 and PIK3CA. Int J Clin Exp Pathol 2015; 8: 10662-10670.

[10] Stolzenburg LR, Wachtel S, Dang H and Harris A. miR-1343 attenuates pathways of fibrosis by targeting the TGF-beta receptors. Biochem J 2016; 473: 245-256.

[11] Fan A, Wang Q, Yuan Y, Cheng J, Chen L, Guo X, Li Q, Chen B, Huang X and Huang Q. Liver X receptor-alpha and miR-130a-3p regulate expression of sphingosine 1-phosphate receptor 2 in human umbilical vein endothelial cells. Am J Physiol Cell Physiol 2016; 310: C216-226.

[12] Liu Y, Li Y, Wang R, Qin S, Liu J, Su F, Yang Y, Zhao F, Wang Z and Wu Q. MiR-130a-3p regulates cell migration and invasion via inhibition of Smad4 in gemcitabine resistant hepatoma cells. J Exp Clin Cancer Res 2016; 35: 19.

[13] Kim GH, Samant SA, Earley JU and Svensson EC. Translational control of FOG-2 expression in cardiomyocytes by microRNA-130a. PLoS One 2009; 4: e6161.

[14] Egawa H, Jingushi K, Hirono T, Ueda Y, Kitae K, Nakata W, Fujita K, Uemura M, Nonomura N and Tsujikawa K. The miR-130 family promotes cell migration and invasion in bladder cancer through FAK and Akt phosphorylation by regulating PTEN. Sci Rep 2016; 6: 20574.

[15] Song W, Zhang Z, Xiao H, Sun S and Zhang H. Roles of epidermal growth factor receptor signaling pathway in silicon dioxide-induced epithelial-mesenchymal transition in human pulmonary epithelial cells. Zhonghua Lao Dong Wei Sheng Zhi Ye Bing Za Zhi 2015; 33: 663-667.

[16] Gagat M, Grzanka D, Izdebska M, Sroka WD, Halas-Wisniewska M and Grzanka A. Tropomyosin-1 protects transformed alveolar epithelial cells against cigaret smoke extract through the stabilization of F-actin-dependent cell-cell junctions. Acta Histochem 2016; 118: 225-235.

[17] Ke XF, Fang J, Wu XN and Yu CH. MicroRNA-203 accelerates apoptosis in LPS-stimulated alveolar epithelial cells by targeting PIK3CA. Biochem Biophys Res Commun 2014; 450: 1297-1303.

[18] Ma C, Li Y, Zeng J, Wu X, Liu X and Wang Y. Mycobacterium bovis BCG triggered MyD88 induces miR-124 feedback negatively regulates immune response in alveolar epithelial cells. PLoS One 2014; 9: e92419.

[19] Grassi G, Di Caprio G, Santangelo L, Fimia GM, Cozzolino AM, Komatsu M, Ippolito G, Tripodi M and Alonzi T. Autophagy regulates hepatocyte identity and epithelial-to-mesenchymal and mesenchymal-to-epithelial transitions promoting snail degradation. Cell Death Dis 2015; 6: e1880.

[20] Tsai WH, Wu CH, Yu HJ and Chien CT. l-Theanine inhibits proinflammatory PKC/ERK/ICAM-1/IL-33 signaling, apoptosis, and autophagy formation in substance P-induced hyperactive bladder in rats. Neurourol Urodyn 2016; [Epub ahead of print].

[21] Zhang S, Niu Q, Gao H, Ma R, Lei R, Zhang C, Xia T, Li P, Xu C, Wang C, Chen J, Dong L, Zhao Q and Wang A. Excessive apoptosis and defective autophagy contribute to developmental testicular toxicity induced by fluoride. Environ Pollut 2016; 212: 97-104.